Magnetocaloric Hydrogen Liquefaction

Jamie Holladay, Kerry Meinhardt, Evgueni Polikarpov, Ed Thomsen, John Barclay (Emerald Energy NW), Corey Archipley (Emerald Energy NW), Jun Cui (PNNL/Ames Lab), Sam Wolf (Ames Lab), and Iver Anderson (Ames Lab)
Pacific Northwest National Laboratory (PNNL)
PO Box 999, MS: K1-90
Richland, WA 99352
Phone: 509-371-6692
Email: Jamie.Holladay@pnnl.gov

DOE Manager: Neha Rustagi
Phone: 202-586-8424
Email: Neha.Rustagi@ee.doe.gov

Subcontractor:
Emerald Energy NW LLC, Redmond, WA

Project Start Date: October 1, 2015
Project End Date: Project continuation and direction determined annually by DOE

Overall Objectives

- Quantify and incorporate novel configurations to achieve simpler, more efficient liquefier designs for liquid hydrogen (LH_2).
- Identify, characterize, and fabricate magnetic materials in shapes suitable for high-performance active magnetic regenerators (AMRs) operating between 280 K and 20 K.
- Fabricate and characterize improved multi-layer magnetocaloric regenerator performance.
- Design, fabricate, test, and demonstrate a lab-scale magnetocaloric hydrogen liquefier.
- Demonstrate a lab-scale hydrogen liquefier that defines how to achieve a figure of merit (FOM) increase from 0.3 up to >0.5 for small commercial liquefiers.
- Perform techno-economic analysis on a 30 metric tons per day of LH_2 liquefier.

Fiscal Year (FY) 2019 Objectives

- Extend calculations of irreversible entropy to explain test results of 8-layer, 4-layer, and 5-layer dual regenerator prototypes and guide path toward designs with FOM >0.60.
- Incorporate lessons learned into the design of a multilayer magnetocaloric hydrogen liquefier (MCHL) stage to span ~285 K to 120 K with sufficient cooling power to precool multilayer stage to span from ~120 K to 20 K and liquefy hydrogen.
- Design new superconducting magnet to provide same field change for all layers of multilayer design and minimize magnetic force imbalance between dual regenerators.
- Develop new pump/circulation subsystem to increase the heat transfer fluid mass flow rates while reducing pressure drops.
- Specify five new magnetic refrigerants for Gen-III (120 K to 20 K operation) and work with Ames Lab to fabricate and characterize five new magnetic refrigerants for 120 K to 20 K.
- Modify rotating disk atomizer to make spherical particles of the five new refrigerants.

Technical Barriers

This project addresses the following technical barrier from the Hydrogen Delivery section of the Fuel Cell Technologies Office Multi-Year Research, Development, and Demonstration Plan[1]:

- (H) High Cost and Low Efficiency of Hydrogen Liquefaction.

Technical Targets

Conventional hydrogen liquefiers at any scale have a maximum FOM of ~0.35 due to intrinsic difficulty of rapid, efficient compression of either hydrogen or helium working gases (depending on liquefier design). The novel approach of this MCHL project uses porous solid magnetic refrigerants cycled in and out of high magnetic fields coupled with heat transfer fluid (HTF) flows to execute an efficient active magnetic regenerative liquefaction (AMRL) cycle that avoids use of gas compressors. Validated numerical modeling of certain scalable high-

[1] https://www.energy.gov/eere/fuelcells/downloads/fuel-cell-technologies-office-multi-year-research-development-and-22

performance AMRL designs indicates they have promise to simultaneously lower installed capital costs per unit capacity and increase thermodynamic efficiency from a FOM of ~0.35 toward ~0.60. Results from experimental prototypes should support the design and deployment of LH_2 plants that meet DOE hydrogen production and delivery targets.

FY 2019 Accomplishments

- Successfully analyzed test results from 1-layer, 4-layer, 5-layer, and 8-layer dual regenerators with helium HTF and actual magnetic field changes at each layer. We found:
  - Irreversible entropy production in each layer from heat transfer between HTF and magnetic refrigerants, viscous dissipation due to pressure drop, and static (no flow) and dynamic (HTF flow) longitudinal conduction is strongly geometry and temperature dependent, which gives different efficiency (coefficient of performance [COP]) for each layer.
  - Increased thermal conductivity due to HTF mixing during flows and direct longitudinal heat conduction heat leak from hot to cold ends of each layer into the cold HTF directly reduce available cooling power/layer.
  - Aspect ratios (axial length [L]/layer diameter [D]) for cylindrical regenerators must be >0.6, which significantly increases overall regenerator length as number of layers increases.
  - Viscous dissipation in multilayer designs dominate irreversible entropy production and limit efficiency even up to helium pressures of ~500+ psia. Liquid HTF such as propane at 200 psia for ~285 K to ~120 K is required for this temperature range; to cool from ~120 K to 20 K, cold He at ~400–500 psia (effectively at ≥1,200 psia when cold) would be used.
- Demonstrated reaching cold temperatures of ~200 K, and successively colder temperatures to ~135 K using 4- or 5-layer regenerators with different amounts of diversion flow of 400 psia He. Results confirm complex coupling among net (available) cooling power and rate of heat rejection curves of *all* layers in a multilayer magnetic regenerator with HTF mass flow rates in each layer.
- Confirmed that in layered reciprocating dual regenerators, force balance between opposing identical regenerators requires adding a specially shaped, high permeability material such as soft Fe for each layer to match total magnetic moments of both regenerators to reduce change in magnetic induction during reciprocating AMR cycle.
- Need new 6.5 T superconducting (s/c) magnet design to give constant high field along ~90% of length of the winding by adding ears to main coil; also has new feature of the same axial field gradient when regenerators leave the high-field region and when they leave the low-field region during the reciprocating stroke. The magnet length is ~50% longer to account for ≥0.6 necessary for higher available cooling power/layer and higher COP/layer.
- Modified helium pump subsystem to use 400 psia He instead of 200 psia.
- Designed a propane HTF circulation system for first stage of the MCHL prototype.
- Fabricated and initially characterized five Gd-Er-Dy-dialuminide refrigerants for use in Gen-III with 120 K to 20 K operation range to make LH_2.
- Modified rotating disk atomization (RDA) apparatus to make spheres of more chemically aggressive dialuminides.

Table 1. PNNL Magnetocaloric Hydrogen Liquefaction Technical Targets

30 tonne/day (small facility)	Claude Cycles (current) [1]	PNNL's MCHL Targets	DOE Target (2017) [1]
Efficiency	<40%	*60%~70%*	85%
FOM	<0.3 (small facility) 0.35~0.37 (large facility)	*~0.6 (small facility)* *~0.65 (large facility)*	0.5
Installed capital cost	$150 million	*$45–$70 million*	~$70 million
O&M cost	4%	*2.8%*	--
Energy input	10-15 kWh/kg H_2	*5~6 kWh/kg H_2*	12 kWh/kg H_2

INTRODUCTION

Claude cycle liquefiers are the current industrial choice for hydrogen liquefaction. They exist as a variety of configurations with processes where helium, hydrogen, or nitrogen gases are refrigerants. These compressors are the largest source of inefficiency in traditional Claude cycle liquefiers. In the case of hydrogen as the refrigerant gas and the process gas, the hydrogen feed to the process is first cooled by liquid nitrogen, and then it is further cooled in counter flow heat exchangers where the cooling power is provided by turbo expansion of a portion of the precooled hydrogen stream. Liquefaction of the precooled, high-pressure hydrogen stream is finally accomplished by throttling in a Joule-Thomson valve into a phase-separator collection vessel. Conventional liquefier technology for hydrogen is limited to an FOM of ~0.35 for a large facility and typically less than 0.3 for a smaller facility.

MCHL technology promises cost effective and more efficient hydrogen liquefaction because it eliminates gas compressors for required work input to the hydrogen process gas and the nitrogen gas making liquid nitrogen to precool the hydrogen. The current MCHL design executes an AMR cycle, which uses reciprocating magnetocaloric materials in and out of regions of high or low magnetic field coupled with HTF to transfer heat between hot and cold thermal reservoirs. The details of the AMR cycle are described in previous annual reports on this project. In essence, the AMR cycle can be highly efficient because magnetization and demagnetization steps are almost reversible; inefficiencies come from irreversible processes in the regenerator. These include finite temperature differences between fluid/solid in convective heat transfer, longitudinal thermal conduction from hot to cold ends of regenerators via several mechanisms, and viscous dissipation during HTF flows. The external parasitic loads, heat rejection loads from adjacent layers/stages, and direct longitudinal heat conduction plus extra work required to reject entropy generated in the regenerator from these three mechanisms all impact layer efficiency and must be included in optimized MCHLs to achieve FOMs of ~0.6. To demonstrate such an efficient device, the MCHL project is modeling, designing, fabricating, and testing multilayer regenerator liquefier designs with fewer magnets and common HTF system, and multistage 1-layer liquefier designs with more magnets and separated HTF systems. Increasing understanding of experimental results and simulation models from several multilayer prototypes led to new s/c magnets, new HTF choices, and better regenerator geometries, which are moving us closer to demonstrating a complete MCHL that spans from ~285 K to ~20 K initially and then demonstrates FOMs of ~0.6.

APPROACH

At a high level the critical path for the MCHL project can be summarized as:

1. Identify, synthesize, and characterize magnetocaloric materials.
2. Develop a database of physical, transport, and thermomagnetic properties for the increasing set of refrigerants with second order phase transitions essential for bypass flow of a portion of cold HTF to continuously cool process gas from room temperature to liquefaction temperature, which increases FOM significantly.
3. Improve magnetic field profile and means to balance large differential forces.
4. Develop HTF subsystems for high-pressure helium and liquid propane use.

5. Investigate multistage and multilayer liquefier designs that incorporate our increasing understanding of the complex coupling of magnetic refrigerants with magnetic field changes and heat transfer fluid flows through regenerators during AMR cycles for efficient performance. Validate designs with detailed performance models and from experimental results.
6. Apply well-known catalysts to efficiently execute ortho-para hydrogen conversion for LH_2; this includes integrating catalysts into compact, microchannel process heat exchangers for 120 K to 20 K stage.
7. Demonstrate microscale LH_2 in one or more MCHL designs to attract industrial partners who want to collaboratively develop small to large LH_2 plants that are cost effective and have FOMs of ~0.60.

The approach is to develop and demonstrate a two-stage, multilayer regenerator design that liquefies hydrogen starting near room temperature. We have several major efforts occurring simultaneously to complete the critical path for this project's research goals.

1. Support Ames Lab's magnetic materials preparation, characterization, and fabrication capabilities. For high-surface-area regenerators, spheres with diameters in the range of 150–250 µm are a good choice. Ames Lab's RDA apparatus can be used to make kilogram batches of spheres with adjustable diameters for different compositions until commercial companies begin to offer such products at competitive prices.
2. Enhance our performance models developed previously and used them to refine our MCHL designs incorporating actual magnet fields, validated magnetic materials, and HTF mass flows in main, diversion, and bypass paths.
3. Develop the HTF circulation subsystem to use liquid propane for the 285 K to 120 K stage and pressurized He for 120 K to 20 K. The safety issues regarding using a flammable liquid as an HTF must be incorporated into the designs. This is not a new method; propane and other light hydrocarbons have been safely used in gas-cycle refrigerators.
4. Pursue proprietary multilayer regenerators in two-stage designs and single-layer regenerators in multistage designs via modeling and experimental efforts. The multilayer regenerators are more complex to design because of the direct coupling among all the layers. This coupled design requires the correct mass of refrigerant in each layer with the corresponding amount of heat transfer fluid flow for each layer must controllable. However, the number of magnets is fewer per liquefier. The 1-layer, multistage liquefiers have independent HTF pumps for each stage, which are simpler and ones we can successfully build now, but at the expense of an HTF pump and 1–2 magnets per stage.

Some of the challenges of multilayer regenerators were tackled in FY 2019 and progress is reported herein. A detailed FOM analysis and updated techno-economic analysis of a 30 tonne/day MCHL were completed in FY 2018.

RESULTS

Analysis of Experimental Results of Several Multilayer Dual Regenerator Prototypes

Magnet Profile

Our existing 7-T superconducting solenoidal magnet has a winding length of 8 in. (20.3 cm) and an inside bore of 5.6 in. (14.2 cm). It is conduction-cooled to ~4 K by a two-stage GM cryocooler with a no-load cooling power of ~ 1.5 W at 4 K and ~50 W at ~40 K. The dual regenerator subsystem operates from ~285 K to ~120 K inside a hermetic stainless-steel tube and the magnet thermal shield at ~50 K to give a maximum regenerator housing diameter of ~3.5 in. (8.9 cm). The axial magnetic field at the center of the magnet decreases to ~60% of peak field at the end of the windings. These dimensions are important for understanding the results of the 8-layer and 4-layer dual regenerator results because the outer-most layer (Gd in these devices) operates from ~240–260 K on the cold end to 280–290 K on its hot end and has to lift the heat rejected from all the colder layers to the temperature set by the external chiller (the only fixed temperature). When the s/c magnet is charged to 6 T for the experiments, the Gd high field is only ~4.2 T and its low field out of the magnet is ~0.3

T. The heat rejection capability of Gd is directly proportional to its adiabatic temperature change for ~3.9 T change instead of a maximum of ~6.0 T. Further, the next two layers colder than Gd (Gd-Dy and Gd-Tb alloys) are both excellent refrigerants that have larger magnetic field changes due to their position nearer the center of the s/c magnet. Hence, their hot and cold adiabatic temperature changes are larger, enabling them to lift more heat to their adjacent hotter layer on to Gd. This illustrates the importance of improving the profile of the s/c magnet to give constant field for ~90% of the winding length.

Regenerator Aspect Ratio

The constraint of the existing s/c magnet diameter and winding length and the maximum total pressure drop of <30 psia for the existing 200 psia HTF pump subsystem required each layer of the 8-layer regenerators to be much shorter than the axial length of original 1-layer Gd magnetic regenerators. These two magnet constraints resulted in L/D aspect ratios as low as ~0.15 in the largest Gd layer in the 8-layer design. The initial cooling results of these dual regenerators at 0.25 Hz and ~6 T maximum field change were very poor and surprising until we analyzed the impact of small aspect ratios on the longitudinal conduction in each layer. Two important insights associated with longitudinal conduction are explained in the equations below. Equation 1 defines the FOM; Equation 2 shows the ideal Carnot work for a refrigerating layer lifting its Q_{dotC} from T_{COLD} to T_{HOT}; and Equation 3 shows the extra work required to reject the irreversible entropy created in the regenerators at T_{HOT}. This real work is in addition to the normal Carnot work required in any refrigerator stage. Equation 3 also shows the external parasitic heat leak and the impact of direct heat transfer due to longitudinal conduction from hot to cold ends of the layer. Hence, there are two effects from longitudinal conduction: the contribution to the S_{IRR} creation and the extra thermal load Q_{dotLC} that must be lifted from T_{COLD} to T_{HOT}. The first of these effects has been included in optimized regenerator design for over three decades, but the second effect has been largely ignored because it was negligible in regenerators with aspect ratios of ~1 (a common geometry). Equation 4 summarizes the major mechanisms inside the regenerators that create irreversible entropy, and Equations 5–8 show equations used to calculate each contribution. Equation 9 is the effective thermal conductivity in the regenerator. Equation 7 and Equation 10 show that the aspect ratio of ~0.15 compared to ~1 increases S_{IRR} and direct conduction heat leak each by ~7 times, which, as shown in Equation 3, increases the real work rate of a layer and reduces the available cooling power of that layer. The extra work increases the rate of heat rejected from a cold layer to the adjacent warmer layer. In the lab-scale prototypes used, a typical case study shows a ~500-g Gd layer's net cooling power is reduced by ~25% by the direct heat leak from longitudinal conduction and also reduces the layer COP by a similar amount. This reduces the cooling power of the Gd layer available to lift heat rejected from the lower layers.

We applied these insights to predict ultimate cold temperature of Gd in dual regenerator AMR prototypes with 1-layer, 4-layer, and 8-layer regenerators. The results are shown in Figure 1 and strongly support our conclusion that the aspect ratio is a key design constraint for any regenerator and is especially important for multilayer regenerators. Our performance models show aspect ratios >0.6 are required to significantly reduce the impact of longitudinal conduction on available cooling and COP. Using this result in conjunction with the use of higher density liquid HTF that reduces S_{IRR} from viscous dissipation, we can achieve COP of each layer of ~0.7, which enables regenerators with multiple layers to achieve FOMs of ~0.6 or more.

$$FOM = \frac{\dot{W}_{ideal}}{\dot{W}_{real}} \quad \text{(Eqn 1)}$$

$$\dot{W}_{ideal_{Layer}} = \dot{Q}_{C_{Layer}} \left(\frac{T_H}{T_C} - 1\right) \quad \text{(Eqn 2)}$$

$$\dot{W}_{real_{Layer}} = \left(\dot{Q}_{CHEX} + \dot{Q}_{LC} + \dot{Q}_{Para}\right)\left(\frac{T_H}{T_C} - 1\right) + \frac{T_H \int_{T_C}^{T_H} \Delta\dot{S}_{IRR} dT}{\int_{T_C}^{T_H} dT} \quad \text{(Eqn 3)}$$

$$\Delta\dot{S}_{IRR} = \Delta\dot{S}_{IRR_{HT}} + \Delta\dot{S}_{IRR_{DP}} + \Delta\dot{S}_{IRR_{LC}} + \Delta\dot{S}_{IRR_{EC}} \quad \text{(Eqn 4)}$$

$$\Delta\dot{S}_{IRR_{HT}} = 2 * \left(\frac{\dot{Q}_{Reg}}{NTU + 1}\left(\frac{1}{T_C} - \frac{1}{T_H}\right)\right) \quad \text{(Eqn 5)}$$

$$\Delta\dot{S}_{IRR_{DP}} = \frac{\dot{m}_{He}}{\rho_{He}} * \frac{\Delta p_{Reg}}{T_H} \quad \text{(Eqn 6)}$$

$$\Delta\dot{S}_{IRR_{LC}} = 2 * \left(\frac{\pi * k_{Reg_{eff}} * D_{Reg}}{4 * a_{ratio}} * \frac{(T_H - T_C)^2}{T_H T_C}\right) \quad \text{(Eqn 7)}$$

$$\Delta\dot{S}_{IRR_{EC}} = 2 * \left\{\left(\frac{16}{5 * \pi}\right)\left(\frac{\pi d_p^{\,2}}{4}\right) * \frac{V_{MM} * v^2 * \Delta B^2}{32 * \rho_{eMM} T_{ave}}\right\} \quad \text{(Eqn 8)}$$

$$k_{Reg_{eff}} = k_{MM_{eff}} + k_{He_{static}} + \rho_{He} c_{p_{He}} D_{L_{Reg}} \quad \text{(Eqn 9)}$$

$$\dot{Q}_{LC} = k_{Reg_{eff}} * \frac{\pi}{4} \frac{D_{Reg}}{a_{ratio}} * (T_H - T_C) \quad \text{(Eqn 10)}$$

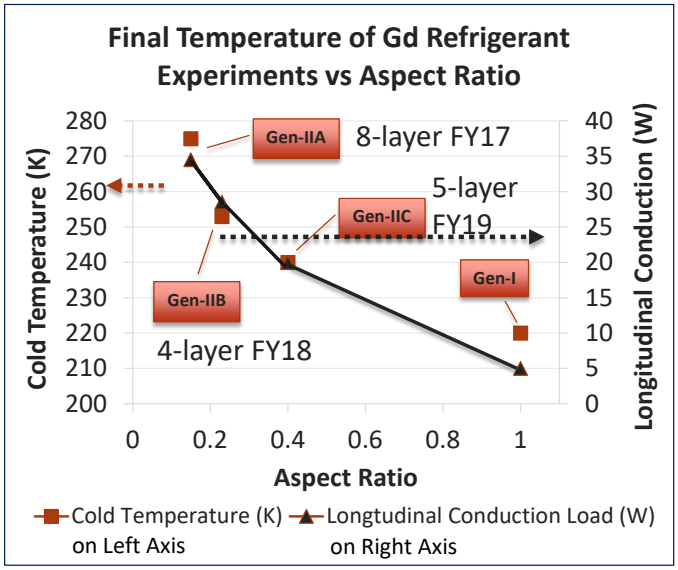

Figure 1. Ultimate cold temperature for a 1-layer (Gen-I), 4-layer (Gen-IIB), 5-layer (Gen-IIC), and 8-layer (Gen-IIA) dual magnetic regenerator MCHL prototypes as function of aspect ratio (L/D) and longitudinal conduction heat leak, which reduces available cooling power.

Improvement to Heat Transfer Fluid System

Helium

The mass flow rate of HTF is a critical MCHL design parameter because the product of its mass flow rate times its heat capacity per unit mass times its average temperature change as it flows through the demagnetized or magnetized regenerators determines the amount of cold cooling power or the rate of hot heat rejection during the two flow steps in an AMR cycle. Our initial HTF subsystem design used He gas at 200 psia (1.38 MPa) with a reciprocating positive displacement pump that produced a maximum mass flow rate at ~0.25 Hz of ~6 g/s. As we increased the mass of magnetic refrigerants in the multilayer regenerators, higher mass flow

rates were required. We successfully purchased a new pump and upgraded the pipe network of the HTF system to use 400 psia (2.76 MPa) with a slightly longer pump stroke to produce a He mass flow rate of ~16 g/s at 0.25 Hz.

Propane

We redesigned the regenerator layers to achieve the desired aspect ratios. After the redesign we calculated the pressure drops from the helium flow rates and found an increased irreversible entropy produced by viscous dissipation during the flow steps of the AMR cycle. Increasing the pressure of helium was considered, but the superior choice was liquid propane. It has a much higher density and thermal mass than helium gas and it has a low enough viscosity to provide to be a good HTF in our magnetic regenerator prototypes, primarily because it has much less viscous dissipation for the required mass flow rates. It doesn't freeze until ~90 K and remains a subcooled liquid at ~290 K at a pressure of ~200 psia (1.38 MPa). It has been suggested in the literature several times, but no one has implemented it to date. We have designed another HTF subsystem to use for the ~285 K to ~120 K first stage of a two-stage multilayer dual regenerator design for a MCHL for LH_2. The second stage from 120 K to 20 K will use cold helium at 400 psia with its ~3+ increase in density compared to near room temperature. The propane HTF system is on our future work list.

New Magnet Features and Specifications

Maximize Refrigerant Performance

Maximum heat rejection capability via HTF flows at T_{HOT} and cooling power at T_{COLD} for magnetic regenerators are directly proportional to ΔT_{HOT} when magnetized and ΔT_{COLD} when demagnetized. These two values are constrained by the first and second laws of thermodynamics for energy and entropy flows via $\Delta T_{COLD} = \Delta T_{HOT}\ \eta\ T_{COLD} / T_{HOT}$ where η includes the effect of S_{IRR} created in the regenerator and has typical values of ~0.40 in inefficient regenerators to ~0.90 in highly efficient regenerators. This constraint is important because it couples the inherent adiabatic temperature change of ferromagnetic refrigerants near their respective Curie temperatures to S_{IRR} creation. To eliminate impact of this condition on layered regenerators where each layer has a different location relative to the center of the magnet, a constant high field profile is required. On a sister project where we are developing an air liquefaction unit, COMSOL AC/DC was used to module to calculate the winding specifications for constant axial magnetic induction over ~90% of a longer magnet including the contributions for the free current (H) and magnetic materials (M). This was accomplished by adding "trim windings" to the ends of the main winding of the magnet. Our new 6.5-T superconducting magnet has a winding length of 11 in. (28 cm), an inside bore of 6.75 in. (17.1 cm), and constant axial field over ~90% of the length of the magnet.

Minimize Magnetic Force Imbalance

A net force from the two opposing attractive forces of the magnetic refrigerants toward the center of the high-field magnet occurs as the regenerators move into and out of the magnetic field. The force on each layer of the multilayer regenerator is the product of its magnet moment (magnetization times its mass divided by its density) times the gradient of the magnetic field along the z axis of the reciprocating motion into/out of the magnet. Hence, to balance forces as one regenerator leaves the high-field region and the other regenerator leaves the low-field region, it is essential to have the same magnetic field gradient at both locations along the z axis. This is not the case for standard solenoids so additional profile shaping is required and has been included in the new magnet design using COMSOL AC/DC. Further, although the total magnetic moments of the opposing dual multilayer regenerators are the same (at the same temperatures), during the reciprocating stroke the largest layer (e.g., 500 g) leaves the high-field region as the smallest layer (e.g., 150 g) leaves the low-field region. This causes a magnetic force difference that requires addition of magnetic material such as soft Fe in the appropriate locations to equalize the distribution of magnetic moment of the regenerators. Details of the force-balancing soft Fe additions were done with COMSOL. With the field gradients the same and equal magnetic moments, the net magnetic force between the dual layered regenerators will be ~0. Of course, as soon as the regenerators begin to cool there will be a relatively small force difference, which is the mechanism for work input into the AMR cycle. This is an important improvement over our previous magnet and addition of soft Fe shapes. The FY 2018 annual report also describes how the force imbalance caused flux jump heating

in the s/c magnet. This negative effect will be minimized in our new magnet and shaping means. We have hedged this conclusion by selecting a cryocooler with 2 W instead of 1.5 W of cooling at 4 K. The new magnet will be integrated with the new cryocooler and cold box as it is manufactured by a qualified and reliable s/c magnet vendor.

135 K Temperature Achieved

Multilayer designs require different magnetic refrigerant masses for each layer because the lifting power of each stage increases to the additional thermal load from the heat rejected from the adjacent colder layer. The different masses/layer immediately requires different HTF mass flow rates/layer for optimum performance. Many of the experiments performed on the 8-layer, 4-layer, and 5-layer regenerators were done with controllable diversion of a portion of the total flow rate into the top layer at the hot end of the regenerators. This T_{HOT} is set by programmable chillers to hold the HTF at ~280–290 K in the regenerators. The details of the innovative diversion flow valves were described in the 2018 annual report. The results from the 8-layer prototype were compromised by the small aspect ratios of the layers, and especially the largest upper two layers. Because of magnet size constraints explained earlier, we reduced the number of layers/regenerators to four refrigerants with Curie temperatures of Gd at 293 K, $Gd_{0.83}Dy_{0.17}$ at 273 K, $Gd_{0.30}Tb_{0.70}$ at 253 K, and $Gd_{0.69}Er_{0.31}$ at 233 K and simultaneously increased the helium HTF pressure to 400 psia. We adjusted the diversion flow valves during the experimental runs and achieved ~200 K as ultimate T_{COLD}. Based on this success, we chose to increase temperature span/layer from 20 K to 30–40 K and use only five layers/regenerator to achieve T_{COLD} of ~120 K. The refrigerants selected had Curie temperatures of 293 K, 253 K, 213 K, 183 K, and 153 K with T_{HOT} of the respective layers of ~285 K, 245 K, 205 K, 175 K, and 145 K. The mass of each layer was adjusted to allow for lower internal efficiency, which increases masses of the upper layers. We ran multiple experiments testing the impact of diversion flow rates on this prototype (Gen-IIC). It was plagued by several leaks in the dual regenerator assembly, mostly due to machine tolerances or failure of HFT seals due to differential thermal contraction as the cold temperatures went below 200 K. To date the prototype has achieved its coldest temperature of 135 K, as illustrated in Figure 2. There is much to learn from experiments on different prototypes to validate our increasing knowledge of MCHL stages to liquefy LH_2 and other cryogens.

Gen-III Final Design

We are waiting for final engineering drawings of the new magnet before we finish the design of the 120 K to 20 K stage (Gen-III) for demonstration of LH_2 production. The original specifications for the magnetic materials for Gen-III assumed 20 K/layer in a 5-layer design with diversion flow between layers 1–2, 2–3, 3–4, and 4–5, and it will have bypass flow to continuously cool the GH_2 process stream. It will use a LN_2 bath with pressure control to hold its temperature at ~120 K. The cold boil-off nitrogen gas from the Gen-III stage will be used to precool the gaseous hydrogen from 285 K to ~120 K. The LN_2 bath will also be used to provide the hot heat sink for the upper layer of Gen-III. Cold helium gas will be the HTF for this stage.

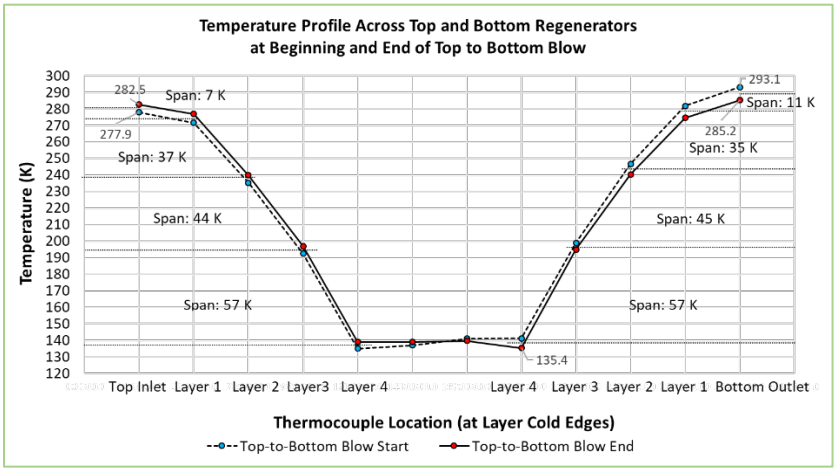

Figure 2. Regenerator temperature profile in Gen-IIC using variations of HTF to achieve ~135 K

RDA Modifications to Make Spheres of Dialuminide Refrigerants for ~153 K to ~43 K

Ames Lab's RDA design was described in FY 2018. It has successfully made spherical powders of 11 different rare earth alloys. Typical size and shape of the RDA rare earth powders are shown in Figure 3. Two major upgrades were carried out and the powder yield has been improved by 30%. One upgrade was on increasing the quench bath size so that liquid metal droplets have extra cooling time before hitting the quenching media and flattening, forming oblates. This upgrade significantly reduced the ratio of nonspherical particles. Another upgrade was on increasing crucible size, which resulted in 70% more loading from 1.5 to 2.5 kg. With these upgrades, RDA can now produce as much as 1 kg (or 990 g) of spherical powder in the desired 150–250 µm size range.

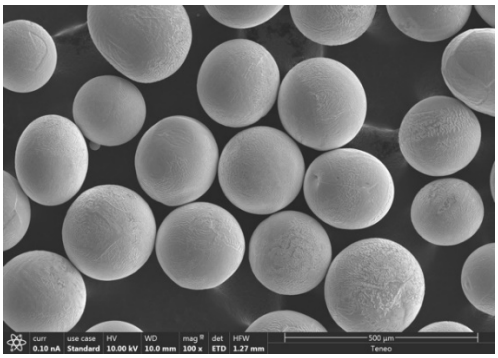

Figure 3. A picture of Gd powders made by RDA showing typical size and shape

Using RDA to manufacture $Gd_xEr_{1-x}Al_2$ spheres was another challenge Ames Lab tackled in FY 2019. It was a challenge because the molten dialuminides reacted with the Ta rotating disc, which works well with alloys containing only rare earth elements. The dialuminides completely reacted with and embrittled the Ta causing the disk to break off and subsequently eroded the low-density machinable alumina supporting disc causing catastrophic failure. Several solutions were attempted, including adding a layer of ceramic oxide to the original disc and a rotating disc entirely made out of zirconia, Zircoa 3001 type, a material which is much more difficult to machine (Figure 4). Different types of zirconia were studied. Our most recent run shows that the zirconia specifically for crucible applications works the best. This disc survived two runs without visible alteration to the surface. The first run used the parameters determined based on the relationship developed by Champagne and Angers [1]. Unfortunately, most of the obtained spherical powders were smaller than the desired size, implying super heat of the melt and disk speed should be adjusted to promote larger powder. In addition, the Ames team ran into a low-yield issue with this new whole zirconia approach. While the zirconia disk provided a stable atomization surface, the additional thermal mass compared to its low-density alumina + thin Ta disk predecessor resulted in a larger material buildup on the disk surface as the disk was brought up to the temperature. In comparison, the thin Ta disk used for rare earth alloys can be quickly brought up to the temperature. It appears that to improve the yield, some form of preheat to the zirconia disc is needed. One solution being investigated now is the graphite susceptor cap concept. The cap is expected to generate the needed heat while the feedstock is being melted. The cap comes off before an atomization run.

Figure 4. Picture of the new rotating disc made of 100% ceramics

CONCLUSIONS AND UPCOMING ACTIVITIES

This project has made progress toward the ultimate goals of increasing the system efficiency while maintaining or decreasing the capital cost of hydrogen liquefaction technologies. In FY 2019 we have made progress along the critical path in that we have:

1. Analyzed results from several multilayer prototypes to understand irreversible entropy production and direct heat leaks into cold HTF from longitudinal conduction
2. Determined that minimum aspect ratios of cylindrical regenerators with spheres is ~0.6
3. Designed specifications for a new superconducting magnet that has very superior characteristics compared to existing standard solenoid magnet
4. Achieved first cool-down and steady state operation of a 5-layer dual active magnetic regenerator refrigerator with a temperature span of 280 K to 135 K
5. Advanced the understanding of how to control HTF flow, the impact of controlling HTF, and the use of diversion flow in layered regenerators
6. Developed innovatively shaped and positioned high-permeability materials for opposing identical multilayer regenerators to almost eliminate magnetic force imbalance in reciprocating MCHL designs
7. Resolved issues with RDA to make spheres of dialuminides for 120 K to 20 K applications
8. Calculated thermomagnetic properties of magnetic refrigerants for 120 K to 20 K.

Upcoming activities will include:

- Finish and certify HTF system for liquid propane
- Finish and test LN_2 precooling apparatus for GH_2 and heat sink for Gen-III
- Complete demonstration of Gen-IIC operation from ~285 K to ~120 K
- Use the lessons learned from Gen-IIB and Gen-IIC to complete the design of the stage two system (Gen-III) operating from 120 K to 20 K
- Characterize and synthesize the remaining dialuminide materials for the second stage
- Build and test the second stage (Gen-III)
- Update the techno-economic analysis prepared in Q4 FY 2018.

FY 2019 PUBLICATIONS/PRESENTATIONS

1. J.A. Barclay, K.P. Brooks, J. Cui, J.D. Holladay, K.D. Meinhardt, E. Polikarpov, and E.C. Thomsen, "Propane Liquefaction with an Active Magnetic Regenerative Liquefier," *Cryogenics* 100, no. 69 (2019). https://doi.org/10.1016/j.cryogenics.2019.01.009.
2. R.P. Teyber, J.D. Holladay, K.D. Meinhardt, E. Polikarpov, E.C. Thomsen, J. Cui, et al., "Performance investigation of a high-field active magnetic regenerator," *Applied Energy* 236, C (2019): 426–436. https://doi.org/10.1016/j.apenergy.2018.12.012.
3. Sam Wolf, Trevor Riedeman, Iver Anderson, Jun Cui, John Barclay, and Jamie Holladay, "Synthesis and Magnetic Performance of Gadolinium Powder Produced with Rotating Disk Atomization Powder Technology," *Powder Technology* 359, no. 1 (January 2020): 331–336. https://doi.org/10.1016/j.powtec.2019.09.035.

4. Corey Archipley, John Barclay, Jamie Holladay, Kerry Meinhardt, Evgueni Polikarpov, and Edwin Thomsen, "Experiments on Cryogenic Multilayer Active Magnetic Regenerative Refrigerators" (prepared for submission to ASME Journal, 2019).
5. J.D. Holladay, K.D. Meinhardt, E.C. Thomsen, E. Polikarpov, J.A. Barclay, C. Archipley, J. Cui, I.E. Anderson, and S. Wolf, "MagnetoCaloric Hydrogen Liquefaction," presented by Jamie D. Holladay at DOE Hydrogen and Fuel Cells Program Annual Merit Review and Peer Evaluation Meeting, Washington, D.C., May 2019.
6. J.D. Holladay and J.A. Barclay, "PNNL's and Emerald Energy NW, Inc. Magnetocaloric Gas Liquefaction Technology," presented by J.D. Holladay to NW Natural LLC, Richland, WA, August 2019.
7. J.D. Holladay, "PNNL's Magnetocaloric Gas Liquefaction Technology," presented by J.D. Holladay to Shell, Richland, WA, May 2019.

REFERENCES

1. B. Champagne and R. Angers, "Size Distribution of Powders Atomized by the Rotating Electrode Process," *Mod. Develop. Powder Metall.* 12 (1980): 83–104.